JOURNAL OF AGRICULTURAL AND FOOD CHEMISTRY
ARTICLE

J. Agric. Food Chem. 2009, 57, 9613–9623 9613
DOI:10.1021/jf901027v

Study of the Evolution of Organic Matter during Composting of Winery and Distillery Residues by Classical and Chemometric Analysis†

Encarnación Martínez-Sabater,§ María A. Bustamante,# Frutos C. Marhuenda-Egea,*,§ Mounir El-Khattabi,§ Raúl Moral,# Emilio Lorenzo,⊥ Concepción Paredes,# Luis N. Gálvez,# and Juana D. Jordá§

§Department of Agrochemistry and Biochemistry, University of Alicante, Apartado 99, E-03080 Alicante, Spain, #Department of Agrochemistry and Environment, Miguel Hernandez University, EPS-Orihuela, Ctra Beniel Km 3.2, 03312 Orihuela (Alicante), Spain, and ⊥Research Technical Services, Alicante University, Spain

The aim of the present paper is to evaluate the changes of organic matter during the composting process of fresh winery and distillery residues (WDR) by means of classical and chemometric analysis of ^{13}C cross-polarization magic angle spinning (CPMAS) NMR and Fourier transform infrared (FT-IR) spectra. ^{13}C NMR spectroscopy displayed a preferential biodegradation of carbohydrates as well as an accumulation of aliphatic chains (cutin- and suberin-like substances). This preferential biodegradation of the organic fractions reduces the landfill emission potential. Although the composition of the input mixture strongly affects the shape of the infrared (IR) spectra, typical bands of components can be selected and used to follow the composting process; that is, changes in the relative absorbances of the band of nitrate (at 1384 cm^{-1}) and in the band of carbohydrates (at 1037 cm^{-1}) have been observed. In addition, different chemometric tools, such as partial least-squares (PLS), interval PLS (iPLS), backward iPLS (biPLS), and genetic algorithm (GA), have been used to find the most relevant spectral region during the composting process. Chemometric analysis based on the combined and sequential use of iPLS and GA has been revealed as a very powerful tool for the detection in samples of the most relevant spectral region related to the composting process. From the obtained results, it can be concluded that CPMAS ^{13}C NMR supported by FT-IR could provide information about the evolution and characteristics of the organic matter during the composting process in order to avoid contamination problems after its use as amendment in agriculture or after landfilling.

KEYWORDS: Compost; organic matter; biodegradation; ^{13}C NMR; FT-IR; partial least-squares; genetic algorithm

INTRODUCTION

Wine production in the European Union represents about 70% of the entire worldwide production (approximately 266.9×10^6 hL), Italy, together with France and Spain, being the major producers (*1*). The winemaking process results in an increasing amount of solid and liquid residues, such as grape stalk (1.907×10^3 t/year), grape marc (5.335×10^3 t/year), wine lees (2.285×10^3 t/year), and winery wastewater and vinasse (162×10^6 m^3/year) (*1*). Composting can constitute a friendly environmental and economical alternative for treating solid organic wastes, such as winery and distillery residues. Composting is defined as a process of aerobic thermophilic microbial degradation, or an exothermic biological oxidation of various wastes, by many populations of indigenous microorganisms, which leads to a stabilized, mature, deodorized, hygienic product, free of pathogens and plant seeds, and rich in humic substances that is easy to store and marketable as organic amendment or fertilizer (*2*−*5*). The composting process is a useful method of producing a stabilized material that can be used as a source of nutrients and soil conditioner in the field (*6*). The nature and properties of the initial mixture are important for the management and understanding of the composting process (*7*). In addition, the composting process involves changes in the physicochemical and chemical characteristics of the composting mixture. For this reason, it is possible to follow the composting process by spectral methods (*5*, *8*, *9*).

Chemometric methods such as partial least-squares regression (PLS) and principal component regression (PCA) have been usually used for the analysis of the NIR and FT-IR spectra (*10*, *11*). However, these methods work with strict orthogonal decomposition, and this decomposition is not realistic, in the

†In memoriam: Jesús Caracuel, Ph.D. (1966−2008), Professor of Geology, Alicante University.

*Author to whom correspondence should be addressed (telephone 965903400, ext. 2063; fax 965903880; e-mail frutos@ua.es.

Published on Web 10/01/2009

sense that the variables or intervals of variables in the original variable space are not interpretable chromophores, fluorophores, or vibraphores (*12*). It would be more interesting to work with methods that select variables or intervals of variables in the original variable space, that is, selecting an interval of the spectrum. This selection in the original spectrum can be interpreted as a chemical species. The spectroscopic information is optimally preserved with iPLS, biPLS, and GA methods (*12*−*15*). iPLS and biPLS methods are new graphically oriented approaches for local regression modeling of spectral data, and GA is a very powerful tool for the variable selection for a PLS model (GA-PLS) (*16*). Making a good selection of the spectral regions and good models, it is possible to improve the predictive ability and, thus, increase the possibilities for the development of new instruments for online monitoring of the process, such as the organic matter evolution during the composting process.

Solid-state ^{13}C nuclear magnetic resonance spectroscopy with cross-polarization and magic angle spinning (CPMAS NMR) allows information to be obtained directly and in a nondestructive way on the carbon components of the entire sample without any chemical or physical fractionation, and it is well suited to the characterization of natural organic matter (*17*−*19*). This technique can be used to detect, and even to quantify, the presence of carbohydrates and alkyl, aromatic, or carboxyl carbons for diverse solid samples such as compost (*5*, *6*, *17*−*27*). Infrared spectroscopy is based on the interaction of infrared light with matter, and it is sensitive to the chemical functional groups present in the sample (*28*, *29*). FT-IR spectroscopy has contributed substantially to the knowledge of the chemistry of soil organic matter (SOM) (*25*, *30*−*33*). The simple sample preparation, the relatively low cost, and the easy accessibility of FT-IR spectroscopy give FT-IR some advantages, such as the possibility of avoiding the potential presence of secondary reactions during sample preparation and that of determining all of the chemical species present in the sample using a unique analysis (*8*). Different composts can be distinguished by their fingerprint region (1500−900 cm^{-1}) (*8*), revealing also in this region fresh and undecomposed materials.

CP-MAS NMR and FT-IR spectroscopies have been used as tools in the study of the composting process (*7*−*9*, *21*−*23*, *27*, *33*). The integration of the CP-MAS spectra of the compost samples showed that the carbon distribution and the modification of these carbon distributions are related to the transformation of the organic matter during the composting process (*33*), that is, the decrease of the carbon distribution in the carbohydrate region (60−110 ppm) during the composting process (*21*, *27*, *33*). With FT-IR spectra, the relative intensity of the typical bands of components can be selected and used to follow the composting process, monitoring the transformation of the organic and inorganic materials (*7*−*9*, *21*). The selection of the regions in CP-MAS spectra or the bands in FT-IR spectra is based on a visual inspection of the spectra. Using multivariate analysis of the spectra we try to find a good correlation between the spectral regions or bands and the composting process. Therefore, the main objective of the present research was to study organic matter transformation during the composting process of fresh winery and distillery residues (WDR), coupling the use of spectral techniques, such as CP-MAS and FT-IR, and chemometric tools (iPLS, biPLS, and GA-PLS).

MATERIALS AND METHODS

Composting Procedure. Three different piles were prepared by the Rutgers static pile composting system, using in all cases wastes from the winery and distillery industry. Pile 1 was prepared with mixtures of grape stalk (GS), grape marc (GM), exhausted grape marc (EGM), and sewage sludge (SS), whereas piles 2 and 3 were elaborated using EGM, cow manure (CM), and poultry manure (PM), respectively (*35*−*37*) (**Table 1**). Sewage sludge came from a treatment plant of municipal wastewater located in Torrevieja (Alicante, Spain). Cow manure was collected from a cattle farm located in Santomera (Murcia, Spain) with a productivity of 35000 heads per year. Poultry manure was collected from a poultry farm with 30000−40000 laying hens located in Orihuela (Alicante, Spain). Grape stalk and GM were collected from a winery located in Jumilla (Murcia, Spain), and EGM was from an alcohol distillery located in Villarrobledo (Albacete, Spain).

Table 1. Characteristics of the Composting Heaps

	pile 1			
waste[a]	initially	after 17 days	pile 2	pile 3
		Composition[b]		
GS	63 (56)	44 (51)		
EGM	25 (28)	18 (25)	70 (80)	70 (79)
GM	12 (16)	9 (15)		
CM			30 (20)	
PM				30 (21)
SS		29 (9)		
		Turning (Days)		
		18−53−86	92	144

[a] GS, grape stalk; EGM, exhausted grape marc; GM, grape marc; CM, cow manure; PM, poultry manure; SS, sewage sludge. [b] Data are expressed as percentage on a fresh weight basis (dry weight basis in parentheses).

The mixtures (about 1800 kg each) were composted in a pilot plant, in trapezoidal piles (1.5 m high with a 2 × 3 m base). The Rutgers static pile composting system was used (*34*), with air supplied by forced aeration, conducted through three basal PVC tubes (3 m length and 12 cm diameter). The aeration system imposed was 30 s every 30 min, with 55 °C as ceiling temperature for continuous ventilation. Compost piles were turned over, when necessary, to improve both homogeneity and the fermentation process (**Table 1**). Forced aeration was used during the bio-oxidative phase, which lasted for 130 days for pile 1, 134 days for pile 2, and 157 days for pile 3. The bio-oxidative phase of composting was considered to be finished when the temperature was close to the external value and reheating did not occur (see Figure S1, Supporting Information). The air blowing was then stopped to allow the composts to mature over a period of approximately 2 months for piles 2 and 3 and 3 months for pile 1. The moisture of the piles was controlled weekly by adding the necessary amount of water to obtain a moisture content of not less than 40%. Excess water, leached from the piles, was collected and added again to the piles. The piles were sampled approximately every 2 weeks during the bio-oxidative phase and after the maturation period. Samples were taken by mixing seven subsamples from seven sites of the pile, from the whole profile (from the top to the bottom of the pile). Each sample was air-dried.

Sample Preparation and Chemical Analysis. Samples were air-dried, ground in an agate mill, then sieved through a 0.125 mm mesh, and milled again with an agate mortar. Total nitrogen (N_T) and total organic carbon (TOC) were determined by automatic microanalysis (*35*) (**Table 2**). The main characteristics of the mixtures at the different sampling times are shown in **Table 3**.

Solid-State ^{13}C NMR and FT-IR Spectroscopy. CPMAS ^{13}C NMR experiments were performed on a Bruker Avance DRX500 operating at 125.75 MHz for ^{13}C. Samples were packed into a 4 mm diameter cylindrical zirconia rotor with Kel-F end-caps and spun at 10000 ± 100 Hz. A conventional CPMAS pulse sequence (*17*) was used with a 1.0 ms contact time. Between 2000 and 5000 scans were accumulated with a pulse delay of 1.5 s. Line broadening was adjusted to 50 Hz. Dipolar dephasing (DD) spectra were generated with a decoupling delay of 45 μs between cross-polarization and data acquisition (*36*). Spectral distributions (the distribution of total signal intensity among various chemical shift ranges) were calculated by integrating the signal intensity in seven

Table 2. Elemental Composition, Total Organic Carbon (TOC), and Total Nitrogen (N_T) of Winery and Distillery Residue Samples Obtained during Composting

treatment time (days)	TOC	N_T	TOC/N_T
Pile 1: Grape Stalk + Grape Marc + Exhausted Grape Marc + Sewage Sludge			
0	48.5	1.3	37.4
17	47.6	2.2	20.9
24	48.6	2.4	20.7
38	48.3	2.2	22.9
52	49.0	2.1	22.9
73	48.0	2.3	21.2
100	47.7	2.2	21.7
234	44.9	2.4	18.8
Pile 2: Exhausted Grape Marc + Cow Manure			
0	49.8	2.4	20.2
15	47.6	2.6	18.5
29	47.3	2.6	18.6
43	47.1	2.7	17.7
50	46.4	2.5	18.7
57	47.4	2.6	18.6
71	47.1	2.6	18.4
85	47.8	2.8	17.1
91	48.1	2.5	19.5
107	45.7	2.7	16.7
114	46.5	2.8	16.9
134	45.2	3.0	15.0
192	46.7	2.9	15.5
Pile 3: Exhausted Grape Marc + Poultry Manure			
0	43.6	3.3	13.1
14	44.5	3.6	12.3
28	42.8	3.7	11.6
42	43.5	3.7	11.9
63	43.7	3.5	12.7
70	43.3	3.2	13.6
90	43.4	3.4	12.8
106	40.3	3.8	10.5
113	40.5	3.8	10.7
133	42.4	3.7	11.5
140	41.9	4.0	10.7
212	42.8	4.1	10.5

chemical shift regions: carbonyl (210−165 ppm), O-aromatic (165−145 ppm), aromatic (145−110 ppm), O_2-alkyl (110−95 ppm), O-alkyl (95−60 ppm), N-alkyl/methoxy (60−45 ppm), and alkyl (45 to −10 ppm) (*37*). The labels indicate only major types of C found in each region.

Spin counting calculation was performed using the method of Smernik and Oades (*38*). Glycine (analytical reagent grade; Sigma) was used as an external intensity standard. The $T_{1\rho}$H and T_1H values were determined as described in Smernik and Oades (*38*). These parameters are very important to avoid signal loss in the CPMAS spectra, because we can choose the best conditions of the CPMAS pulse sequence (these experimental conditions are described above). The percentage of potential ^{13}C NMR signal, which was actually observed (C_{obs}), was in the range of 60−66% for the CPMAS technique (*38*). The main source of error was uncertainty in the integrated NMR intensities. Two replicate measurements were carried out for all samples.

The FT-IR spectra were collected on a Bruker IFS 66 spectrometer. The resolution was set to 4 cm^{-1}, and the operating range was 400−4000 cm^{-1}. Samples (7−10 mg) were mixed with 100 mg of dried KBr, and then the mixture was pressed into pellets. In all cases, 20 scans per sample were recorded, averaged for each spectrum, and corrected against the spectrum with ambient air as background.

Chemometric Analysis. The iPLS, biPLS, and GA-PLS analyses, especially useful for wavelength selection, have been used. These algorithms have been already described (*12*−*16*), and the reader is referred to these papers for more details. To reach the best model with the lowest cross-validated error, the models and preprocessing methods (none, scaling, multiplicative scatter correction (MSC), and extended multiplicative signal correction (EMSC)) (*39*) were tested.

Table 3. Evolution of the Main Parameters during the Composting Process (Dry Weight Basis)[a]

composting time (days)	pH	EC (dS m^{-1})	OM (%)	C_{org} (g kg^{-1})	N_T (g kg^{-1})	C_{HA} (%)	C_{FA} (%)
Pile 1: Grape Stalk + Grape Marc + Exhausted Grape Marc + Sewage Sludge							
0	4.67	4.21	91.7	485	12.9	8.0	5.4
16	7.42	1.93	89.0	476	22.3	2.4	3.6
24	7.36	1.86	87.9	486	23.6	3.2	3.3
38	7.34	1.72	88.2	483	21.6	2.4	3.6
52	7.49	2.07	88.5	490	21.3	3.0	3.4
59	7.39	1.92	87.2	483	22.7	2.4	3.6
73	7.23	1.77	86.6	480	22.6	2.6	4.0
86	7.35	1.94	84.9	475	22.4	2.7	3.6
100	6.99	2.08	86.5	477	22.1	1.3	3.4
116	7.12	1.74	86.9	501	23.0	1.9	3.6
130	7.06	1.94	84.8	538	26.5	1.6	3.8
234	7.01	2.75	84.3	449	24.0	1.3	2.7
Pile 2: Exhausted Grape Marc + Cow Manure							
0	7.08	1.96	88.5	498	23.6	3.6	1.9
15	7.28	2.26	87.6	476	25.7	6.2	1.8
29	7.14	2.57	87.0	473	25.9	4.2	1.7
43	7.12	2.67	87.1	471	26.6	4.2	1.6
50	6.79	2.95	86.4	464	24.8	3.9	1.6
57	6.87	2.41	87.2	474	25.7	3.3	1.5
71	6.95	2.71	86.1	471	26.0	2.7	1.5
85	6.94	2.74	84.8	478	28.0	3.6	1.5
91	6.95	2.59	85.6	481	25.1	2.6	1.5
107	7.16	2.92	83.1	457	27.4	3.1	1.3
114	7.20	2.92	84.2	465	27.8	2.8	1.3
134	7.03	2.75	81.5	452	29.8	2.6	1.4
192	7.38	2.82	82.0	467	29.1	2.7	1.4
Pile 3: Exhausted Grape Marc + Poultry Manure							
0	7.48	2.12	82.3	436	33.0	3.3	2.0
14	7.13	3.01	81.6	445	36.5	4.6	1.7
28	7.05	3.09	80.3	428	36.8	2.3	1.6
42	7.03	2.66	79.1	435	36.9	2.4	1.6
63	6.89	2.87	79.3	438	34.9	2.9	1.3
70	6.85	2.82	79.3	433	32.1	2.2	1.3
90	6.86	3.12	74.6	434	34.3	2.2	1.4
106	7.12	3.09	75.4	403	38.3	3.1	1.4
113	7.17	2.94	74.0	405	37.9	2.8	1.3
133	7.21	2.86	74.1	424	37.4	2.8	1.4
140	7.31	2.48	73.6	419	39.8	2.4	1.3
212	8.14	2.34	73.9	428	41.2	2.1	1.2

[a] EC, electrical conductivity; OM, organic matter; C_{org}, total organic C; N_T, total N; C_{HA}, humic acid-like C; C_{FA}, fulvic acid-like C.

Software. MATLAB version 6.5 from MathWorks was used for the calculations, and iToolbox (including methods for iPLS, biPLS, and dynamic biPLS), EMSC Toolbox (for preprocessing methods), and GA-PLS Toolbox are available at http://www.models.kvl.dk.

RESULTS AND DISCUSSION

Solid-State CPMAS ^{13}C NMR Spectroscopy. The NMR observable carbon content (C_{obs}) can be measured in the samples using the spin counting methodology (*38*). Using this methodology, C_{obs} was around 60−66% in our WDR compost samples. These values indicate that some signal is being under-detected; however, this situation does not represent a problem, provided that all of the undetected carbon is equally representative across all carbon forms (*38*, *40*). The problem appears when there is

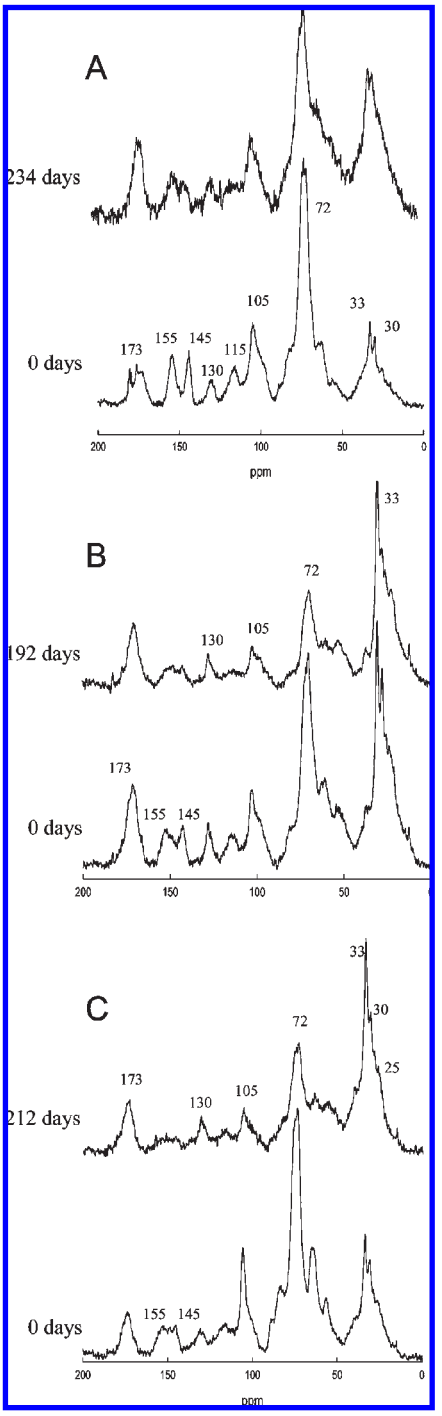

Figure 1. Solid-state CPMAS ^{13}C NMR spectra of compost of pile 1 (**A**), pile 2 (**B**), and pile 3 (**C**).

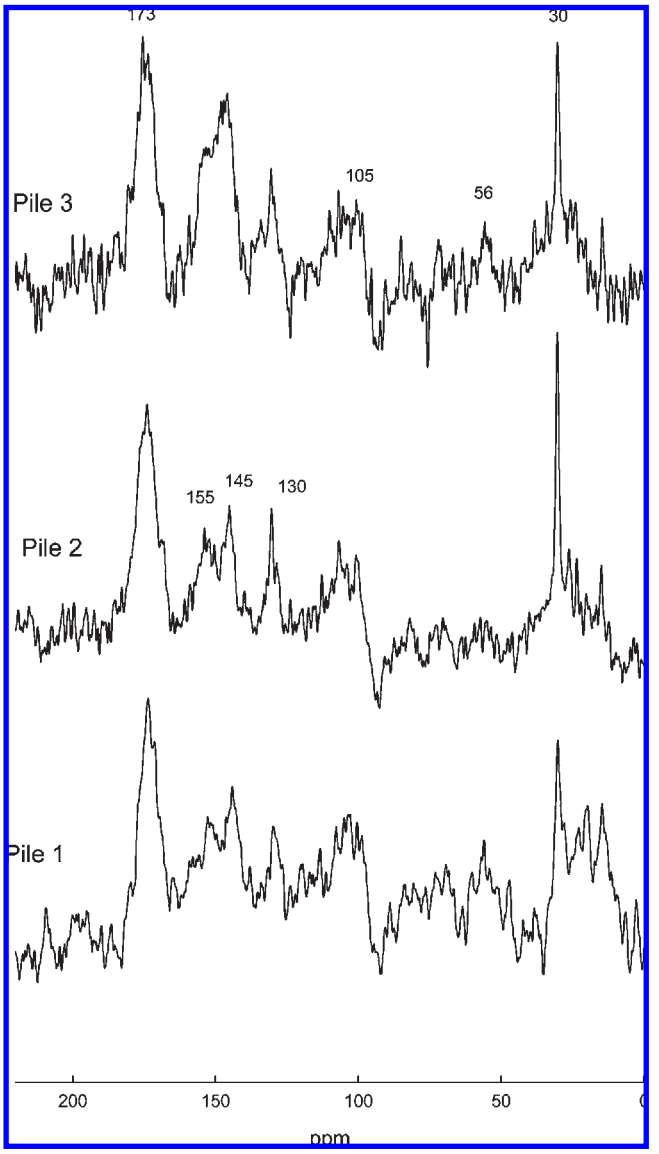

Figure 2. RMN dipolar dephasing (DD) ^{13}C NMR spectra of compost for pile 1 (grape stalk + grape marc + exhausted grape marc + sewage sludge), for pile 2 (exhausted grape marc + cow manure), and for pile 3 (exhausted grape marc + poultry manure).

some selectivity in the detection of carbon. Therefore, comments about the relative quantities of different forms of organic matter must be treated with caution (*40*). The CPMAS ^{13}C NMR spectra show several main peaks corresponding to the samples collected at the beginning of the composting process (**Figure 1**): 173, 155, 145, 130, 115, 105, 72, 65, 56, 33, and 30 ppm. A shoulder appears around 25 ppm in CPMAS spectra and also in DD spectra (**Figure 2**), indicating the presence of methyl groups in alkyl chains. The methyl group presents an elevated mobility and, therefore, a weak coupling (*36*). At 30 and 33 ppm we found the methyl and methylene groups, respectively. The main difference between the methyl and methylene groups is related to carbon dipolar interactions with linked protons. As a result, a peak appears in DD spectra at 30 ppm. On the contrary, methylene groups (33 ppm) present a strong coupling and disappear in DD spectra (**Figure 2**). These assignments have been reported in other works (*7*, *41*−*46*) and for the DD spectra.

The peak that appears around 56 ppm in CPMAS spectra was lost in DD spectra, supporting the assignment to C_α of polypeptides (*42*). The signal at 56 ppm disappears in DD spectra because the coupling of the C_α with the linked proton is strong (**Figure 2**). However, the signal at 56 ppm in CPMAS spectra can be also assigned to $O-CH_3$ groups in lignin (phenolmethoxyl of coniferyl and sinapyl moieties) and in hemicellulose (glucoronic acid in xylan) (*23*). The WDR compost principally derived from plant and organic remains, and it contains different biomolecules, such as proteins and peptides, as well as lignin and hemicellulose. Thus, the signal around 56 ppm has contribution from C_α of polypeptides and $O-CH_3$ groups in lignin and in hemicellulose (*47*). Signals around 72−74 ppm, assigned to cellulose and hemicellulose in CPMAS spectra, disappear in the DD spectrum.

The chemical shift at 105 ppm has been assigned to different carbons of lignin-type moieties in CPMAS spectra: the C2

carbons of both guaiacyl and syringyl lignin structures and the C6 carbon of syringyl units. This peak is also attributed to quaternary aromatic carbons in tannins (*19*, *36*). Chemical shifts in this region do not appear in the DD spectrum for pile 3 (**Figure 2**). In the DD spectrum for pile 2 (**Figure 2**) a signal appears around 105 ppm. A contribution from quaternary carbons, probably tannins, supports this assignment. However, the low signal-to-noise (S/N) ratio in these spectra makes difficult the assignment.

The region of the CPMAS spectrum between 110 and 170 ppm can be divided in two subregions: the first region between 110 and 140 ppm is attributed to unsubstituted aromatic C and C-substituted aromatic carbons (*44*). The second region between 140 and 160 ppm is assigned to aromatic carbons linked to O or N. The first region exhibits well-defined peaks at 115 and 130 ppm. The peak around 130 ppm is characteristic of unsubstituted aromatic C, including C1 quaternary carbons of syringyl and guaiacyl lignin units and the C6 carbon of guaiacyl (*45*). The second subregion between 140 and 160 ppm shows peaks traditionally assigned to lignin or tannins (*19*, *36*). The peak centered at 145 ppm is attributed to methoxy- or hydroxy-substituted phenyl C (*7*, *36*). The peak at 155 ppm is assigned to oxygen-substituted aromatic C, including both C−OCH_3 and C−OH groups (*36*, *45*). This peak could also be assigned to C4 carbons of guaiacyl units involved in ether linkages to C_β of adjacent lignin units. In the DD spectra, in the subregion between 140 and 160 ppm, it is possible to find two peaks at 145 and 155 ppm (**Figure 2**). These peaks indicate a large contribution of tannins (*45*).

The region between 170 and 200 ppm in the CPMAS spectra is assigned to carbonyl/carboxyl carbons of ester and amide groups (*7*, *45*). The contribution of amides at the signals in this region should be large, because the nitrogen content is high (**Table 2**). In this way, the peak intensity at 173 ppm increases in the CPMAS spectrum from pile 1 after the addition of sewage sludge N-rich component (**Tables 1** and **2**).

Changes in C Compounds Shown by Solid-State CPMAS ^{13}C NMR Spectroscopy. Figure 3 shows the evolution of the C content in the seven regions of the NMR spectra. The main C types are O-alkyl (95−60 ppm) and alkyl (45 to −10 ppm). These two regions suffer opposite evolutions throughout time. The O-alkyl (from cellulose and hemicellulose) signals decrease with composting time. In all of the piles the intensity of the alkyl signals (from aliphatic chains, such as lipids, cutin, or suberin) increases in the mature compost. Aliphatic structures of cutin and suberin molecules are resistant to biodegradation, and they could have been accumulated throughout the composting process (*27*, *41*). This is a concentration effect over the C-alkyl by a preferential degradation of sugar polymer, such as cellulose and hemicellulose, during the composting process (*27*). Minor components in the CPMAS spectra of the compost samples are carbonyl (210−165 ppm), O-aromatic (165−145 ppm), aromatic (145−110 ppm), O_2-alkyl (110−95 ppm), and N-alkyl/methoxy (60−45 ppm) (*37*). The contribution of these minor components in the CPMAS spectra is also shown in **Figure 3**. The scatter of the data (**Figure 3**) could reflect the nonquantitative characteristic of the CPMAS technique, as the errors show (the observable carbon contents for the WDR compost samples were generally around 60−66%).

Applying the method established by Nelson et al. (*46*), we can determine the contribution of different biomacromolecules (carbohydrate, protein, lignin, aliphatic material, char, and pure carbonyl) in total organic matter (bearing in mind that the observable carbon contents for the WDR compost samples were generally around 60−66%) of different compost samples (*47*). It is reasonable to accept the hypothesis that all organic matter in compost is constituted by biomacromolecules (*47*). According to

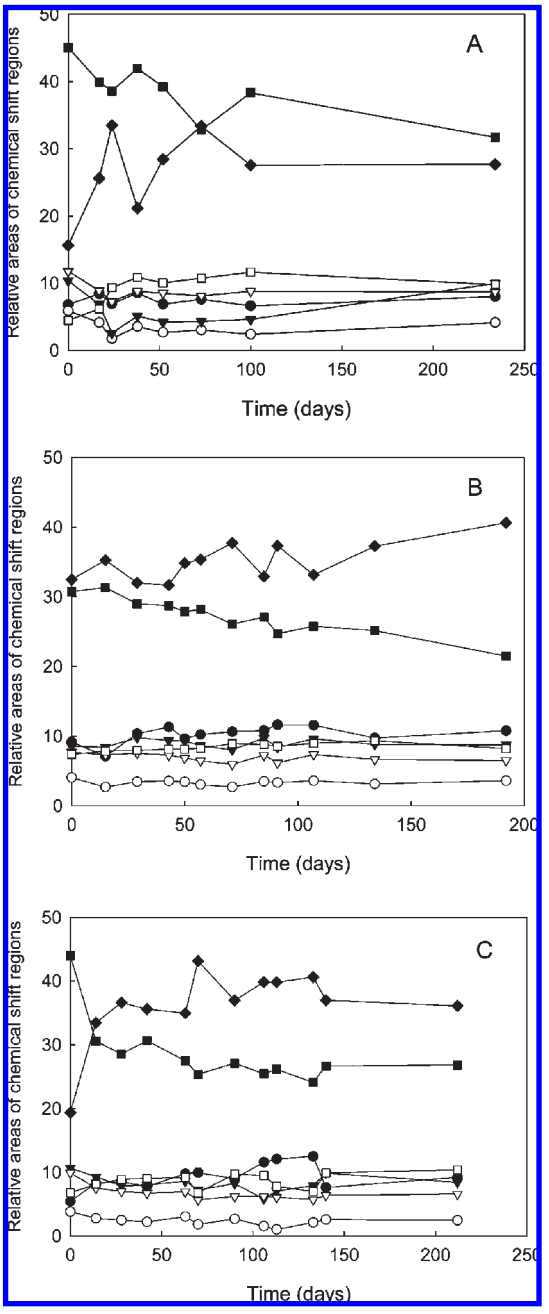

Figure 3. Evolution of the C content in the seven regions of the NMR spectra of the composting samples of pile 1 (**A**), pile 2 (**B**), and pile 3 (**C**). The symbols correspond to the following regions in ppm: (●) 210−165; (○) 165−145; (▼) 145−110; (▽) 110−95; (■) 95−60; (□) 60−45; (◆) 45 to −10.

Nelson et al. (*46*, *47*), 90% of biomolecules can be classified as carbohydrates (A), protein (B), lignin (C) and aliphatic structures (D). The results obtained after applying the model to our data are shown in **Figure 4**. In both piles 2 and 3, a decrease of the content of carbohydrates was observed during the composting process, as well as an increase of protein and aliphatic material. The composting process is related to a high microbial activity, and the microbial enrichment (*8*) could determine the increase in the protein content in the composting piles. The degradation of carbohydrates is mainly produced due to the breakdown of the C−O linkage. To analyze possible relationships between the variations in the components of the piles, a stepwise linear regression analysis was performed using SPSS software v. 12

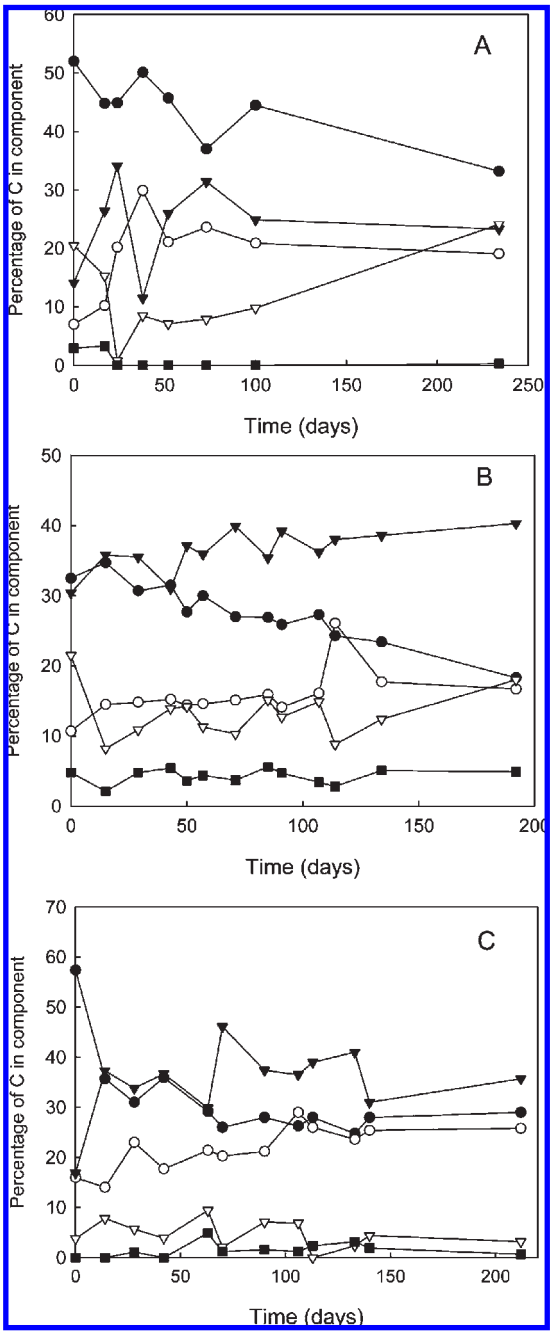

Figure 4. Predicted molecular composition of organic carbon, using CP NMR analysis, of the composting samples of pile 1 (**A**), pile 2 (**B**), and pile 3 (**C**). The symbols correspond to the following biomolecules: (●) carbohydrates; (○) proteins; (▼) aliphatic; (▽) lignin; (■) carbonyl.

(see Table S1, Supporting Information). For the carbohydrate variation, aliphatic is the first variable included in the model for piles 2 and 3. Carbohydrates were also related to proteins in pile 3. No correlations were obtained for pile 1.

Piles 2 and 3 maintained temperatures above 40 °C for 76 and 122 days, respectively. Moreover, the temperature within these piles reached higher values (above 50 °C). However, pile 1 showed variable temperatures during the composting process. At the beginning of the process the maximum temperature values were reached (see Figure S1, Supporting Information), but it decreased quickly and the pile needed to be enriched with sewage sludge after 17 days to improve the composting process (**Table 1**). Turning operations were necessary to increase the temperature of pile 1. This behavior could suggest that the organic matter was not stabilized enough, and this fact could lead to contamination problems after its use as amendment in agriculture or after landfilling. However, the nuclear magnetic resonance data displayed a good stabilization degree of the organic matter in pile 1. The carbohydrates decreased and the aliphatic material increased (**Figure 4**). Probably, the raw materials used are the key in the compost production, because these initial materials will determine the behavior of the compost pile and the necessary operations to reach a good stabilization degree of the organic matter. We can conclude that the evolution of the organic matter in the compost piles is a very complex process, and not only a degradation of certain biomolecules and the accumulation of others. On the other hand, the reduction in the carbohydrate content can suggest a reduction of the emission potential of final stable compost, although the lack of a longer thermophilic stage may cause sanitation problems.

Evaluation of the Composting Process by FT-IR Spectra. FT-IR was used to monitor the composting process, evaluate the degradation rate, and thus determine the maturity. Although the composition of the initial mixture strongly affects the shape of the infrared (IR) spectra (**Figure 5**), typical bands of components can be selected and used to follow the decomposition process (*8*). Evaluation of the composting processes can be based on the changes of the band relative intensity (see Figure S2, Supporting Information). This is in agreement with a conclusion made by Provenzano et al. (*48*), which reports that the FT-IR spectra of organic matter during composting are qualitatively similar but differ in the relative intensity of absorbance bands.

All FT-IR spectra were characterized by a number of absorption bands, exhibiting variable relative intensities, and showed the changes of functional groups of compounds that characterize different stages of decomposition of fresh winery and distillery residues (**Figure 5**) (*7*, *33*). The stretching vibration of bonded OH groups and water causes a broadband at around 3400 cm^{-1} (*7*–*9*). Peaks at 2927 and 2854 cm^{-1} are attributed to aliphatic methylene groups in aliphatic chains (*49*). Due to their general presence and the relationship of their decrease to the decomposition of waste materials, these bands could be very useful for comparing composting processes. The band at 1640 cm^{-1} reflects the absorption of aromatic C═C vibrations and C═O in carboxylates, amide I, and OH bending vibrations from water, and is adsorbed by functional groups in organic matter and inorganic constituents (*50*). The band in the region 1510−1550 cm^{-1} can be assigned to amide II and components containing lignin. These bands are identified in biowastes due to their content of wood and plants that are rich in lignin (*51*). A broadband was found at around 1420 cm^{-1} due to the OH in-plane bend of carboxylic acids, the CO_2 stretch of carboxylates, and the aliphatic CH_2 group of alkanes. The band at 1384 cm^{-1} is assigned to nitrate. Additional bands were also observed at 1260 cm^{-1}, which correspond to the C−O stretching of aryl ethers and phenols and C−O and O−H bending of carboxylic groups. Around 1154 cm^{-1} there were alcoholic group vibrations (*52*). The absorbance in the FT-IR spectra of different fresh winery and distillery residues (**Figure 5**) in the region 1100−1030 cm^{-1} was assigned to C−O stretching of polysaccharides or polysaccharide-like substances. An intense broad absorption band appears in the characteristic carbohydrate region with maxima at 1096 and 1037 cm^{-1} assigned to vibrations of C-3−H−O-3−H and C-6−H_2−O-6−H of cellulose groups and pyranosyl-ring vibrations, and 1154 cm^{-1} was assigned to asymmetric stretching of C−O−C of the glycosidic link (*53*).

Inorganic components such as carbonates absorb at 875 cm^{-1}, and phosphate absorbs between 600 and 500 cm^{-1}. The sharp nitrate band appears exclusively at a later phase (**Figure 5**).

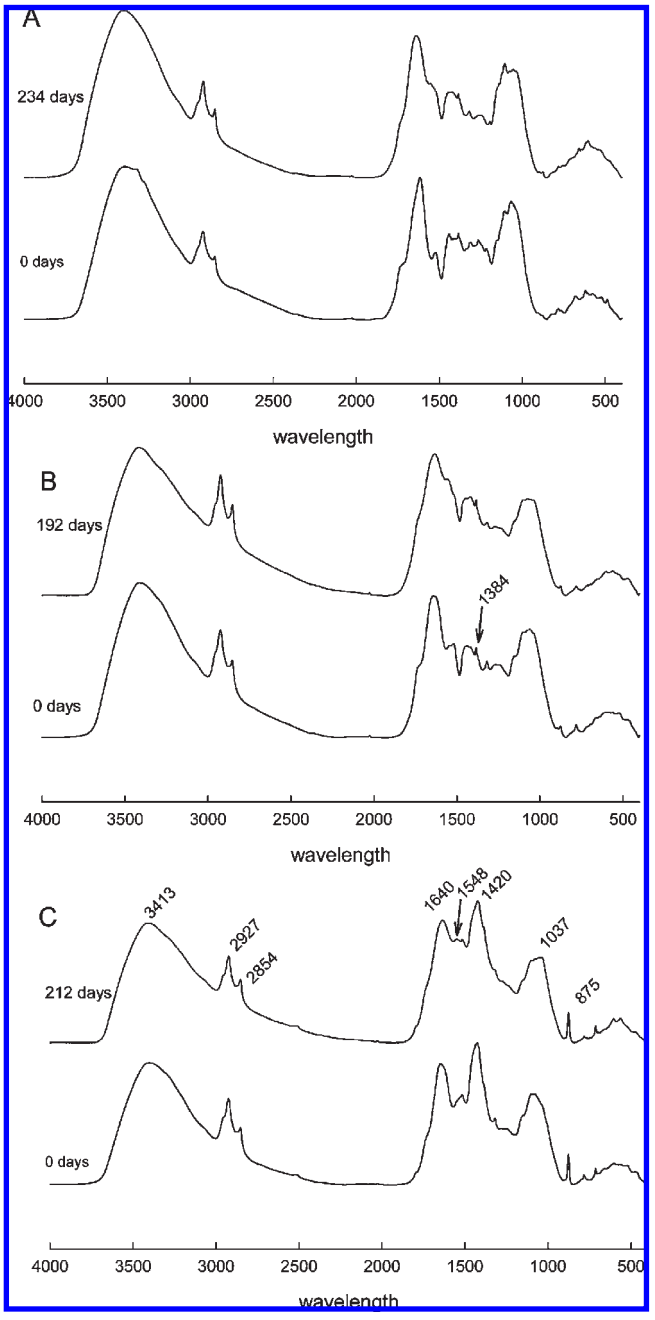

Figure 5. FT-IR spectra of initial composting mixture and spectra of fresh and mature compost of pile 1 (**A**), pile 2 (**B**), and pile 3 (**C**).

Its wavenumber position is stable and highly reproducible at 1384 cm^{-1}. Its presence indicates the state of decomposition at which the nitrogen derived from decomposed components is oxidized. Inorganic compounds (silica, silanol, carbonate, nitrate, phosphate) exhibit very prominent and reproducible bands. Inorganic bands can be easily distinguished from organic bands by their size and shape. Due to the relative increase of the inorganic part during the composting process, the corresponding bands enlarge as well.

Certain characteristic bands that represent the input material and the composting process were selected to determine the relative absorbances. The relative absorbance (rA) is the height of one distinct band multiplied by 100 and divided by the sum of all compared band heights (*54*). Band heights were measured and corrected referring to the chosen baseline by OMNIC 5.1b software. Seven bands were used to calculate relative absorbances (rA): 2927, 2854, 1640, 1548, 1420, 1384, 1037, and 875 cm^{-1}. The course of relative absorbances reflects the progress of decomposition. Changes of relative absorbances of the bands at 1384 and 1037 cm^{-1} were observed (see Figure S2, Supporting Information). An increase of relative absorbance at 1384 cm^{-1} took place during decomposition in the first stages, and afterward decreases when the compost reaches maturity in piles 2 and 3 (see Figure S2, Supporting Information). A weak nitrate band appeared in the spectra of the first day compost samples for pile 3 and the intensity band decreased after 70 days, probably because nitrogen was utilized by the microorganisms of the composting mixture. Koivula and Hanninen (*55*) showed that the nitrogen content was higher in all humic fractions of the old bale and could be an indicator of microbial enrichment (**Table 2**). As microbes die, their nitrogen becomes available to living microbes, and microbial utilization of cellulose may intensify with time.

The increase in the relative absorbance at 1548 cm^{-1} can be related to the increase in the protein content in the piles as shown by CPMAS ^{13}C NMR spectroscopy (**Figure 1**). On the other hand, a slight decrease of relative absorbance at 1037 cm^{-1} was observed during composting (see Figure S2, Supporting Information). This is in agreement with the studies of the whole compost FT-IR spectra carried out by Hsu and Lo (*56*), who also showed that easily degradable organic matter components, such as polysaccharides, are decomposed and, therefore, the mature compost contains a greater number of aromatic structures of higher stability. These results suggest the occurrence of degradation and condensation reactions of organic structures.

In conclusion, spectral analyses, such as solid-state NMR and FT-IR, are very good tools to evaluate the evolution of organic matter during composting. On the other hand, it is very important to know the nature of the raw materials used in the mixture, because it will determine the behavior of the compost pile. The complexity of the composting process involves the degradation and transformation of the more labile organic molecules, by the action of the microorganisms, into more recalcitrant forms. In the compost piles presented here, elaborated using wastes from the winery and distillery industry by the Rutgers static pile composting system, the composting process was characterized by a preferential degradation of the polysaccharides.

Evaluation of the Composting Process by Multivariate Analysis of the Spectroscopic Data. To obtain optimal information, qualitative and quantitative, from spectroscopic data a multivariate chemometric evaluation should be included in the research work. For this reason PLS regression was applied to the NMR and FT-IR measurements in relation to the composting time. Full-spectrum PLS models were performed on the four separate sample sets (^{13}C NMR and FT-IR for piles 2 and 3). The only problem was the low number of samples collected throughout the composting process; that is, analysis for pile 1 was not performed due to the lack of a sufficient number of samples. With piles 2 and 3 we had enough measurements to carry out a good multivariate analysis. The results for all models performed (**Table 4**) show the values with respect to root-mean-square error of cross-validation (RMSECV). In the same way, we modeled our spectroscopic data with the composting time and not with a chemical component present in the samples, as it is the most common situation (*12*−*16*). Our main interest was to locate the most informative spectral regions during the composting process. To locate these regions, iPLS regression and biPLS regression were carried out. Twenty equidistant intervals were tested on the spectroscopic data (**Table 4**).

Table 4. Fully Cross-Validated PLS, iPLS, biPLS, and GA-PLS Models for Prediction of Composting Time from ^{13}C NMR and FT-IR Spectra by Piles 2 and 3

method	preprocessing	components	intervals	RMSECV	*r*
			CPMAS ^{13}C NMR Pile 2		
PLS	EMSC	6	0−200[b]	7.79	0.981
iPLS[a]	EMSC	5	140−150[b]	8.85	0.974
biPLS[a]	EMSC	6	20−30,[b] 30−40,[b] 100−110,[b] 140−150[b]	7.41	0.983
			FT-IR Pile 2		
PLS	MSC	5	4000−600[c]	12.59	0.956
iPLS[a]	MSC	4	1569.8−1432.9[c]	10.35	0.965
biPLS[a]	MSC	3	3577.3−3438.5,[c] 3295.8−3156.9,[c] 3155.0−3018.1,[c] 1569.8−1432.9[c]	9.93	0.967
GA-PLS			1569.8−1556.3,[c] 1517.7−1508.1,[c] 1496.5−1483.0[c]	3.72	
			CPMAS ^{13}C NMR Pile 3		
PLS	EMSC	4	0−200[b]	16.04	0.935
iPLS[a]	EMSC	2	50−60[b]	20.91	0.880
biPLS[a]	EMSC	6	10−20,[b] 40−50,[b] 50−60,[b] 170−180[b]	9.84	0.975
			FT-IR Pile 3		
PLS	MSC	4	4000−600[c]	20.34	0.879
iPLS[a]	MSC	4	2973.7−2805.9[c]	15.72	0.931
biPLS[a]	MSC	4	2973.7−2805.9,[c] 1616.1−1448.3,[c] 1106.9−939.2[c]	18.25	0.906
GA-PLS		13	2962.1−2954.4,[c] 2906.2−2904.3,[c] 2879.2−2871.5,[c] 2867.6−2865.7,[c] 2840.6−2836.8[c]	4.80	

[a] In this model, the spectra were divided in 20 intervals. [b] NMR intervals in ppm. [c] FT-IR intervals in cm^{-1}.

Figure 6 shows full cross-validated prediction errors for the 20 interval biPLS models (bars) for ^{13}C NMR for piles 2 and 3. The biPLS models for piles 2 and 3 using four intervals performed better than the full spectrum model or the iPLS model (**Table 4**). The biPLS model for ^{13}C NMR for piles 2 and 3 showed the intervals correlated with the composting time (**Figure 6**). For pile 2, the intervals are in the alkyl region (45 to −10 ppm), in the O_2-alkyl region (110−95 ppm), and in the O-aromatic region (165−145 ppm) (**Table 4**). As shown with a more classical analysis of the spectroscopy data (see above), the content of aliphatic or aromatic molecules is very important in the composting process of pile 2. For pile 3, the intervals are in the alkyl region (45 to −10 ppm), in the N-alkyl/methoxy region (60−45 ppm), and in the carbonyl region (210−165 ppm) (**Table 4**).

The iPLS models for FT-IR displayed good values of RMSECV by piles 2 and 3, only with an interval (**Table 4**). The improvement working with more intervals (biPLS models) was not high with the FT-IR data; it was better than the iPLS model for pile 3. For pile 2, the interval was 1432.9−1569.8 cm^{-1}, and in these regions we can find the components of lignins and aromatic C=C binding. For pile 3, the interval was 2805.9−2973.7 cm^{-1}, this region being the alkyl region. By applying genetic algorithms (GA-PLS) in these regions, it is possible to improve the models for a better prediction capacity (**Table 4**). In other words, we can determine the wavelength interval more correlated with the composting process. The spectra for the final samples of the composting process (192 days for pile 2 and 212 days for pile 3) were not considered in the calculations. The air blowing was then stopped to allow the composts to mature over a period of approximately 2 months. In the two maturation months the alterations of the organic matter were very small and there was no correlation with the composting time. Probably, between the two final samples, the organic material in the compost piles did not undergo alterations, and it can be considered that the organic material was stable.

With the intervals selected by iPLS method, the GA-PLS method can be applied for wavelength selection (*16*). We have worked only with the FT-IR spectra for piles 2 and 3. We tried to carry out the GA-PLS method with NMR spectra, but the low signal/noise ratio did not allow this chemometric approach. GA-PLS applied on the interval selected by iPLS method in the FT-IR spectra from pile 2 produced a RMSECV of 3.72% (selecting 3 regions and 7 components) (**Table 4**). For pile 3, the same strategy produced a RMSECV of 4.80% (selecting 5 regions and 13 components) (**Table 4**). This approach using sequentially iPLS and GA-PLS improved significantly the predictive ability, as shown by the decrease in the RMSECV values (**Table 4**). In a classical study of the spectroscopic data, the usual strategy is to work with the peaks, but after the chemometric approach it can be seen that the wavelengths selected are not always the highest peaks (**Table 4**).

In conclusion, the classical analysis of the spectroscopic data from ^{13}C NMR and from FT-IR techniques allows one to follow and evaluate organic matter evolution during the composting process of fresh winery and distillery residues. In this process, the initial composition of the compost piles was very important for the understanding of the preferential degradation of the different biomolecules. However, the more common situation was a preferential degradation of the carbohydrates and an increase of the aliphatic material (probably by a concentration effect in the compost pile).

On the other hand, with the chemometric approach it is possible to go more in depth into the knowledge of the composting process. It was possible to model the composting process with good RMSECV values by sequential application of iPLS and GA-PLS. Interval PLS removes the noninformative intervals, and the genetic algorithm can work with a significantly lower number of variables. With this strategy, it is possible to select a few wavelengths in the FT-IR spectra with a high correlation with the composting process to determine when the organic matter is stable in a composting pile.

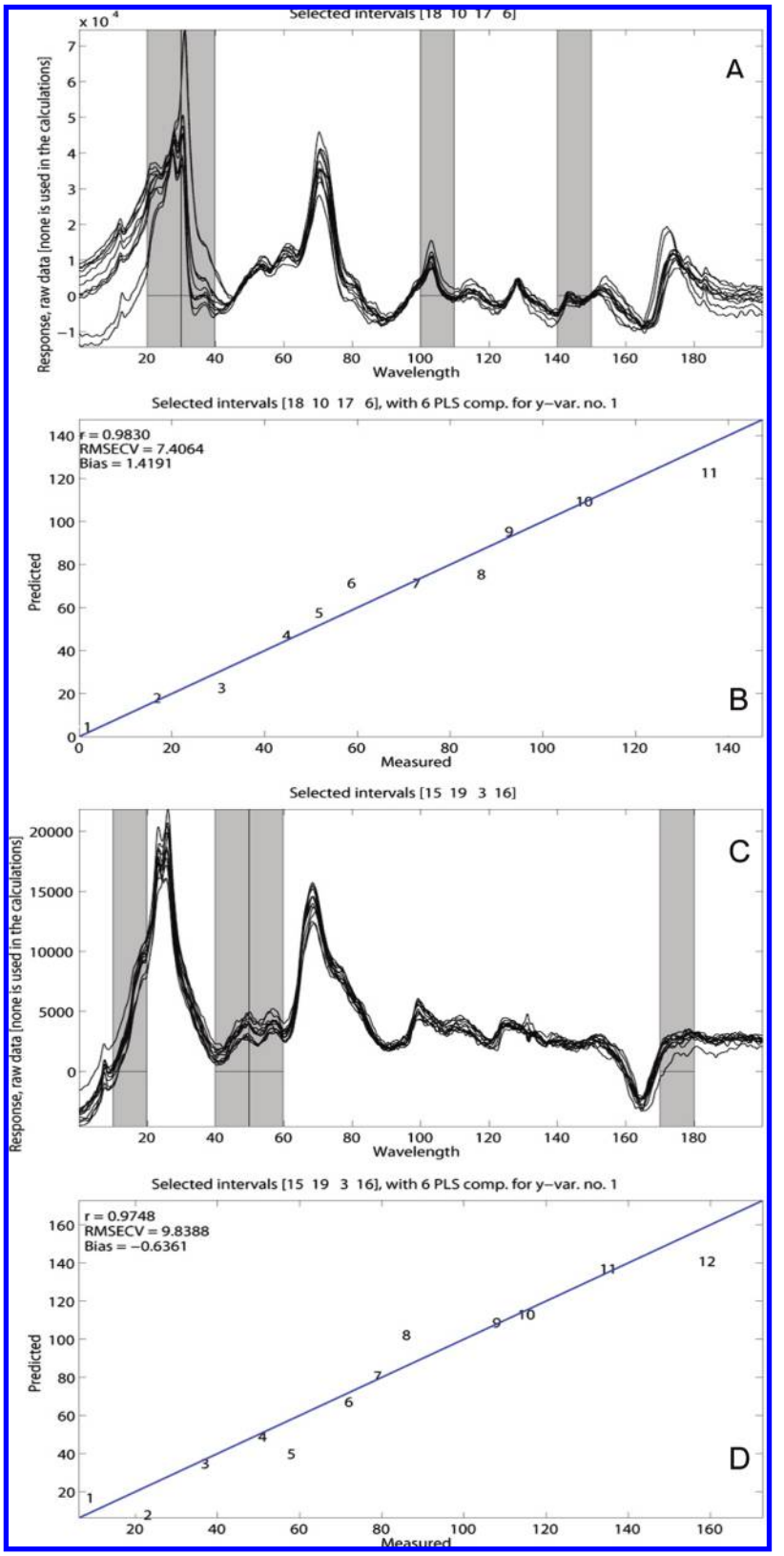

Figure 6. (**A**) Four intervals included in the optimal PLS model of ^{13}C NMR data by pile 2: 20−30, 30−40, 100−110, and 140−150 ppm. (**B**) Predicted versus measured composting time for this model by pile 2. (**C**) Four intervals included in the optimal PLS model of ^{13}C NMR data by pile 3: 10−20, 40−50, 50−60, and 170−180 ppm. (**D**) Predicted versus measured composting time for this model by pile 3.

Supporting Information Available: Table S1 and Figures S1 and S4. This material is available free of charge via the Internet at http://pubs.acs.org.

LITERATURE CITED

(1) OIV. State of the Vitiviniculture World Market; *Organisation Internationale de la Vigne et du Vin*, **2009**; available at http://www.oiv.int.

(2) Stevenson, F. J.; He, X. T. Nitrogenin humic substances as related to soil fertility. In *Humic Substances in Soil and Crop Sciences*; MacCarthy, P., Clapp, C. E., Malcolm, R. L., Bloom, P. R., Eds.; Selected Readings; Soil Science Society of America and American Society of Agronomy: Madison, WI, 1990; pp 91−109l.
(3) Haug, R. T. *The Practical Handbook of Compost Engineering*; CRC Press: Boca Raton, FL, 1993; p 2
(4) Ouatmane, A.; Provenzano, M. R.; Hafidi, M.; Senesi, N. Compost maturity assessment using calorimetry, spectroscopy and chemical analysis. *Compost Sci. Util.* **2000**, *8*, 124–134.
(5) Pichler, M.; Knicker, H.; Kogel-Knabner, I. Changes in the chemical structure of municipal solid waste during composting as studied by solid-state dipolar dephasing and PSRE ^{13}C NMR and solid-state ^{15}N NMR spectroscopy. *Environ. Sci. Technol.* **2000**, *34*, 4034–4038.
(6) Castaldi, P.; Alberti, G.; Merella, R.; Melis, P. Study of the organic matter evolution during municipal solid waste composting aimed at identifying suitable parameters for the evaluation of compost maturity. *Waste Manag.* **2005**, *25*, 209–213.
(7) Inbar, Y.; Chen, Y.; Hadar, Y. Carbon-13 CPMAS NMR and FTIR spectroscopic analysis of organic matter transformations during composting of solid wastes from wineries. *Soil Sci.* **1991**, *152*, 272–282.
(8) Grube, M.; Lin, J. G.; Lee, P. H.; Kokorevicha, S. Evaluation of sewage sludge-based compost by FT-IR spectroscopy. *Geoderma* **2006**, *130*, 324–333.
(9) Smidt, E.; Eckhardt, K.; Lechner, P.; Schulten, H.; Leinweber, P. Characterization of different decomposition stages of biowaste using FT-IR spectroscopy and pyrolysis-field ionization mass spectrometry. *Biodegradation* **2005**, *16*, 67–79.
(10) Martens, H.; Jensen, S. A. Partial least squares regression: a new two stage NIR calibration method. In *Cereal Chemistry and Technology*; Holas, J., Kratochvil, J., Eds.; Elsevier: Amsterdam, The Netherlands, 1983.
(11) Norris, K. H. *Near Infrared Technology in Agricultural and Food Industries*; American Association of Cereal Chemist: St. Paul, MN, 1987.
(12) Norgaard, L.; Saudland, A.; Wagner, J.; Nielsen, J. P.; Munck, L.; Engelsen, S. B. Interval partial least-squares regression (iPLS): a comparative chemometric study with an example from near-infrared spectroscopy. *Appl. Spectrosc.* **2000**, *54*, 413–419.
(13) Winning, H.; Viereck, N.; Norgaard, L.; Larsen, J.; Engelsen, S. B. Quantification of the degree of blockiness in pectins using ^{1}H NMR spectroscopy and chemometrics. *Food Hydrocolloids* **2007**, *21*, 256–266.
(14) Norgaard, L.; Hahn, M. T.; Knudsen, L. B.; Farhat, I. A.; Engelsen, S. B. Multivariate near-infrared and Raman spectroscopy quantifications of the crystallinity of lactose in whey permeate powder. *Int. Dairy J.* **2005**, *15*, 1261–1270.
(15) Leardi, R.; Lupiáñez González, A. Genetic algorithms applied to feature selection in PLS regresión: how and when to use them. *Chemom. Intell. Lab. Syst.* **1998**, *41*, 195–207.
(16) Leardi, R.; Norgaard, L. Sequential application of backward interval partial least squares and genetic algorithms for the selection of relevant spectral regions. *J. Chemom.* **2004**, *18*, 486–497.
(17) Wilson, M. A. *NMR Techniques and Applications in Geochemistry and Soil Chemistry*; Pergamon Press: Oxford, U.K., 1987.
(18) Preston, C. Applications of NMR to soil organic matter analysis: history and prospects. *Soil Sci.* **1996**, *161*, 144–166.
(19) Preston, C. M.; Trofymow, J. A.; Niu, J.; Fyfe, C. A. ^{13}CPMAS-NMR spectroscopy and chemical analysis of coarse woody debris in coastal forests of Vancouver Island. *For. Ecol. Manag.* **1998**, *111*, 51–68.
(20) Baldock, A.; Oades, J. M.; Nelson, P. N.; Skene, T. M.; Golchin, A.; Clarke, P. Assessing the extent of decomposition of natural organic materials using solid-state C-13 NMR spectroscopy. *Aust. J. Soil Res.* **1997**, *35*, 1061–1083.
(21) Chen, Y. N. Nuclear magnetic resonance, infra-red and pyrolysis: application of spectroscopic methodologies to maturity determination of composts. *Compost Sci. Util.* **2003**, *11*, 152–168.
(22) Tang, J.-C.; Maie, N.; Tada, Y.; Katayama, A. Characterization of the maturing process of cattle manure compost. *Process Biochem.* **2006**, *41*, 380–389.
(23) Gómez, X.; Diaz, M. C.; Cooper, M.; Blanco, D.; Morán, A.; Snape, C. E. Study of biological stabilization processes of cattle and poultry manure by thermogravimetric analysis and C-13 NMR. *Chemosphere* **2007**, *68*, 1889–1897.
(24) Kögel-Knabner, I.; Hatcher, P. G. Characterization of alkyl carbon in forest soils by CPMAS ^{13}C NMR spectroscopy and dipolar dephasing. *Sci. Total Environ.* **1989**, *81*/*82*, 169–177.
(25) Stevenson, F. J. Extraction, fractionation and general chemical composition of soil organic matter. In *Humus Chemistry*; Stevenson, F. J., Ed.; Genesis, Composition, Reactions; Wiley: New York, 1982.
(26) Nip, M.; Tegelaar, E. W.; de Leeuw, J. W.; Schenck, P. A.; Holloway, P. J. A new non-saponifiable highly aliphatic and resistant biopolymer in plant cuticles. *Naturwissenschaften* **1986**, *73*, 579–585.
(27) Almendros, G.; Dorado, J.; Gonzáles-Vila, F. J.; Blanco, M. J.; Lankes, U. ^{13}C NMR assessment of decomposition patterns during composting of forest and shrub biomass. *Soil Biol. Biochem.* **2000**, *32*, 793–804.
(28) Hesse, M.; Meier, H.; Zeeh, B. *Spektroskopische Methoden in der organischen Chemie*; Georg Thieme Verlag: Stuttgart, Germany, 1995.
(29) Smith B. *Infrared Spectral Interpretation*; CRC Press: Boca Raton, FL, 1999.
(30) Schnitzer M.; Khan, S. U. *Humic Substances in the Environment*; Dekker, New York, 1972.
(31) MacCarthy, P.; Rice, J. A. Spectroscopic methods (other than NMR) for determining functionality in humic substances. In *Humic Substances in Soil Sediment, and Water*; Aiken, G. R., McKnight, D. M., Wershaw, R. L., MacCarthy, P., Eds.; Wiley: New York. 1985
(32) Gerasimowicz, W. V.; Byler, D. M. Carbon-13 CPMAS NMR and FTIR spectroscopic studies of humic acids. *Soil Sci.* **1985**, *139*, 270–278.
(33) Inbar, Y.; Chen, Y.; Hadar, Y. Solid state carbon 13 nuclear magnetic resonance and infrared spectroscopy of composted organic matter. *Soil Sci. Soc. Am. J.* **1989**, *53*, 1695–1701.
(34) Finstein, M. S.; Miller, F. C.; Mac Gregor, S. T.; Psariamos, K. M. *The Rutgers Strategy for Composting: Process Design and Control*; EPA Project Summary (EPA 600/S2-85/059); U.S. Environmetal Protection Agency: Washington, DC.1985
(35) Navarro, A. F.; Cegarra, J.; Roig, A.; Bernal, M. P. An automatic microanalysis method for the determination of organic carbon in wastes. *Commun. Soil Sci. Plant Anal.* **1991**, *22*, 2137–2144.
(36) Preston, C. M. Carbon-13 solid-state NMR of soil organic matter-using the technique effectively. *Can. J. Soil Sci.* **2001**, *81*, 255–270.
(37) Baldock, J. A.; Smernik, R. J. Chemical composition and bioavailability of thermally, altered *Pinus resinosa* (red pine) wood. *Org. Geochem.* **2002**, *33*, 1093–1109.
(38) Smernick, R. J.; Oades, J. M. The use of spin counting for determining quantitation in solid state ^{13}C NMR spectra of natural organic matter. 2. HF-treated soil fractions. *Geoderma* **2000**, *96*, 159–171.
(39) Martens, H.; Nielsen, J. P.; Engelsen, S. B. Light scattering and light absorbance separated by extended multiplicative signal correction. Application to near-infrared transmission analysis of powder mixtures. *Anal. Chem.* **2003**, *75*, 394–404.
(40) Patti, A. F.; Issa, J.; Wilkinson, K. *What are putting on the ground? Characterisation of grape marc and other composts used in the Yarra Valley*; Grape and Wine Research and Development Corporation, Australia Government: 2004.
(41) Vane, C. H.; Drage, T. C.; Snape, C. E. Bark decay by the white-rot fungus *Lentinula edodes*: polysaccharide loss, lignin resistance and the unmasking of suberin. *Inter. Biodeter. Biodegr.* **2006**, *57*, 14–23.
(42) Mathers, N. J.; Xu, Z.; Blumfield, T. J.; Berners-Price, S. J.; Saffigna, P. G. Composition and quality of harvest residues and soil organic matter under windrow residue management in young hoop pine plantations as revealed by solid-state ^{13}C NMR spectroscopy. *For. Ecol. Manag.* **2003**, *175*, 467–488.
(43) Veeken, A. H. M.; Adani, F.; Nierop, K. G. J.; de Jager, P. A.; Hamelers, H. V. M. Degradation of biomacromolecules during high-rate composting of wheat straw-amended feces. *J. Environ. Qual.* **2001**, *30*, 1675–1684.

(44) Kögel-Knabner, I. The macromolecular organic composition of plant and microbial residues as inputs to soil organic matter. *Soil Biol. Biochem.* **2002**, *34*, 139–162.
(45) Keeler, C.; Kelly, E. F.; Maciel, G. E. Chemical−structural information from solid-state ^{13}C NMR studies of a suite of humic materials from a lower montane forest soil, Colorado, USA. *Geoderma* **2006**, *130*, 124–140.
(46) Nelson, P. N.; Baldock, J. A.; Oades, J. M.; Churchman, G. J. Dispersed clay and organic matter in soil: their nature and associations. *Aust. J. Soil Res.* **1999**, *37*, 289–315.
(47) Nelson, P. N.; Baldock, J. A. Estimating the molecular composition of a diverse range of natural organic materials from solid-state ^{13}C NMR and elemental analyses. *Biogeochemistry* **2005**, *72*, 1–34.
(48) Provenzano, M. R.; de Oliveira, S. C.; Silva, M. R. S.; Senesi, N. Assessment of maturity degree of composts from domestic solid wastes by fluorescence and Fourier transform infrared spectroscopies. *J. Agric. Food Chem.* **2001**, *49*, 5874–5879.
(49) Réveillé, V.; Mancuy, L.; Jardé, E.; Garnier-Sillan, E. Characterisation of sewage sludge derived organic matter: lipids and humic acids. *Org. Geochem.* **2003**, *34*, 615–627.
(50) Smidt, E.; Meissl, K. The applicability of Fourier transform infrared (FT-IR) spectroscopy in waste management. *Waste Manag.* **2007**, *27*, 268–276.
(51) Smidt, E.; Lechner, P.; Schwanninger, M.; Haberhauer, G.; Gerzabek, M. H. Characterization of waste organic matter by FT-IR spectroscopy—application in waste science. *Appl. Spectrosc.* **2002**, *56*, 1170–1175.
(52) Ait Baddi, G.; Hafidi, M.; Cegarra, J.; Alburquerque, J. A.; Gonzálvez, J.; Gilard, V.; Revel, J.-C. Characterization of fulvic acids by elemental and spectroscopic (FTIR and ^{13}C-NMR) analyses during composting of olive mill wastes plus straw. *Bioresour. Technol.* **2004**, *93*, 217–323.
(53) Bower, D. I.; Maddams, W. F. *Vibrational Spectroscopy of Polymers*; Cambridge University Press: Cambridge, U.K., 1989.
(54) Haberhauer, G.; Rafferty, B.; Strebl, F.; Gerzabek, M. H. Comparison of the composition of forest soil litter derived from three different sites at various decompositional stages using FTIR spectroscopy. *Geoderma* **1998**, *83*, 331–342.
(55) Koivula, N.; Hanninen, K. Concentrations of monosaccharides in humic substances in the early stages of humification. *Chemosphere* **2001**, *44*, 271–279.
(56) Hsu, J. H.; Lo, S. L. Chemical and spectroscopic analysis of inorganic matter transformations during composting of pig manure. *Environ. Pollut.* **1999**, *104*, 189–196.

Received September 16, 2008. Revised manuscript received September 15, 2009. Accepted September 16, 2009. This work has been supported by grants from the Ministerio de Educación y Ciencia of Spain and has been financed by the CICYT (AGL2002-00296) Project, from the Generalitat Valenciana (GVPRE/2008/208) Project, and from the University of Alicante (GRJ0508) and (UAUSTI07-02) Projects.